Desalination and Water Treatment
www.deswater.com

doi: 10.1080/19443994.2015.1088479

57 (2016) 18529–18536
August

Taylor & Francis
Taylor & Francis Group

Tannin modified aminated silica as effective absorbents for removal of light rare earth ions in aqueous solution

Yue-yue Shen[a], Rui-lin Yang[a], Yang Liao[a,b], Jun Ma[a,b], Hui Mao[a,b,*], Shi-lin Zhao[a,b,*]

[a]*College of Chemistry and Materials Science, Sichuan Normal University, Chengdu, Sichuan 610068, China, emails: shen028@163.com (Y.-y. Shen), 1484682653@qq.com (R.-l. Yang), 153796826@qq.com (Y. Liao), 1044208419@qq.com (J. Ma), Tel./Fax: +86 02884761393; emails: rejoice222@163.com (H. Mao), zhaoslin@aliyun.com (S.-l. Zhao)*
[b]*The Engineering Center for the Development of Farmland Ecosystem Service Function, Sichuan Normal University, Chengdu, Sichuan 610068, China*

Received 20 May 2015; Accepted 25 August 2015

ABSTRACT

A series of novel absorbents (SiO_2-BT, SiO_2-BWT and SiO_2-BT and BWT) were prepared by immobilizing plant tannins onto amine-modified silica. The as-prepared absorbents were characterized by field emission scanning electron microscopy and Fourier transform infrared spectrometer. Subsequently, the absorbents were utilized for the removal of Pr^{3+} and Nd^{3+} from aqueous solution. We systematically investigated the influences of pH values, initial concentration of metal on the adsorption capacity, as well as the adsorption kinetics and adsorption isotherms. The obtained experimental results suggested that among these absorbents, SiO_2-BT exhibited the best performances for the removal of both Pr^{3+} and Nd^{3+} in aqueous solutions. Under the optimum conditions, the adsorptive removal efficiency could reach the adsorption equilibrium just within 60 min, and the adsorption capacities of Pr^{3+} and Nd^{3+} on SiO_2-BT were 329.2 and 341.5 mg/g, respectively. It was found that the adsorption kinetics was well described by the pseudo-second-order kinetic model while the adsorption isotherms followed the Langmuir adsorption model.

Keywords: Tannin; Aminated silica; Light rare earth ions; Adsorptive removal

1. Introduction

Rare earth, known as the vitamin of industry, has been widely used in many fields of modern society to improve the material properties, such as permanent magnets [1], catalytic activity [2], optical parameter [3], metal, and conductivity [4]. During these applications, it is inevitable to generate a large amount of rare earth ions contaminated aqueous solutions, which may cause potential threats to people's health and environmental safety, if not properly handled [5,6]. To address this concerned issue, it is essentially important to find an effective approach to remove rare earth ions from aqueous solutions.

Various approaches have been proposed for the removal of rare earth ions from aqueous solutions, such as ions exchange [7], extraction chromatography [8], solvent extraction [9], and absorption [10]. Among these methods, adsorption is one of the most attractive techniques that is able to effectively remove pollutants with low concentration in aqueous solutions [11]. As a consequence, great effort has been dedicated to

*Corresponding authors.

developing novel adsorbents with high adsorption capacity and fast adsorption rate to cost-effectively solve the pollution problems caused by rare earth ions in aqueous solutions.

Tannins are natural polyphenols, which can be easily obtained by extraction from leaves, fruits, and barks of plants [12]. Tannins have abundant adjacent phenolic hydroxyls on their molecules, which exhibit high chelating ability towards various metal ions with empty d-orbital [13,14]. However, tannins are water-soluble compounds, which need immobilization onto solid matrices before their practical applications [15–17]. The already reported tannin-based adsorbents have been successfully utilized to remove Au^{3+}, uranium, and Cr^{6+} from aqueous solutions, while there is still an absence in the investigations on rare earth removal. The existence of wastewater containing rare earth ions could lead to environmental pollution if not properly handled. Therefore, it is extremely urgent to deal with the rare earth ions in water. Based on these considerations, we attempted to use tannin adsorbents for the removal of rare earth ions from aqueous solutions. Silica has good mechanical, thermal, and chemical stability [18]. Hence, silica could be the ideal supporting matrix to prepare tannin-immobilized adsorbents with good physical and chemical properties.

In this work, two typical tannins, bayberry tannin (BT) and black wattle tannin (BWT) were immobilized onto silica to prepare three adsorbents (SiO_2-BT, SiO_2-BWT and SiO_2-BT and BWT). Subsequently, the as-prepared absorbents were characterized by FTIR and scanning electron microscopy (SEM). Subsequently, these absorbents were used for the removal of Pr^{3+} and Nd^{3+} from aqueous solutions. The adsorption removal behaviors were systematically investigated under different experimental conditions. It should be noted that in the present investigation, we highlight the use of low-cost plant tannins as adsorption biomass for the effective removal of light rare earth ions from aqueous solutions, which features high adsorption capacity to the rare earth ions. Another advantage of our strategy is the employment of SiO_2 as supporting matrices, which significantly improves the adsorption kinetics by providing the target rare earth ions easy access to the immobilized phenolic hydroxyls. Compared with already reported activated carbon materials based on physical adsorption mechanism [19], our prepared organic–inorganic functional composites materials exhibited substantially improved adsorption capacity. With regard to the adsorption kinetics, our adsorbents show obvious advantages in comparison with anion exchange resin [20]. Consequently, we provided a cost-effective and facile approach for the effective removal of light rare earth ions from aqueous solutions.

2. Materials and methods

2.1. Reagents

Bayberry tannin (BT) and black wattle tannin (BWT) were obtained from the barks of *Myrica esculenta* and black wattle tree, respectively. Pr_2O_3 (CAS: 12036-32-7) was used as the source of praseodymium ions, while Nd_2O_3 (CAS: 1313-97-9) was used as neodymium ions. All main reagents were of analytical grade.

2.2. Preparation of absorbents

2.2.1. Preparation of aminated mesoporous silica (NH_2-SiO_2)

NH_2-SiO_2 was prepared by a method similar to the literature [21]. Cyclohexane (CAS: 110-82-7), *n*-hexanol (CAS: 25917-35-5), and Triton X-100 (CAS: 9002-93-1) (4:1:1, V/V) were mixed with constant stirring for 30 min. Then, moderate deionized water was added into the mixture under constant stirring (10:1, deionized water: Tritonx-100). After 30 min, an emulsion was formed. Tetraethyl orthosilicate (TEOS) (CAS: 78-10-4) (5 mL) and silane coupling agent KH-550 (CAS: 919-30-2) were added into the emulsion, followed by vigorous stirring for another 30 min. Then, a proper amount of $NH_3 \cdot H_2O$ (CAS: 1336-21-6) was dropped in and kept under vigorous stirring for 24 h. Acetone (CAS: 67-64-1) and anhydrous ethanol (CAS: 67-17-5), used as emulsion breakers, were added into the emulsion. Finally, NH_2-SiO_2 was obtained by filtration, extensively washed with deionized water, and dried in vacuum.

2.2.2. Preparation of bayberry tannin-immobilized aminated silica (SiO_2-BT) and black wattle tannin-immobilized aminated silica (SiO_2-BWT)

0.5 g of BT was dissolved in 100 mL of deionized water and mixed with 1.0 g NH_2-SiO_2 prepared in Section 2.2.1. 10 mL of glutaraldehyde was added into the mixture which was stirred at 40℃ for 6 h. The pH was adjusted to 2.0, followed by stirring for 24 h. The SiO_2-BT adsorbent was prepared by filtration, fully washed with deionized water, and dried at 40℃ for 24 h in vacuum.

For the preparation of SiO_2-BWT, other experimental conditions were the same as those adopted for the preparation of SiO_2-BT except that the amount of used

BWT was 0.1 g. In the case of SiO_2-BT and BWT, 0.2 g of BT and 0.2 g of BWT were used for the synthesis.

2.2.3. Characterizations

The absorbents were characterized by infrared spectrum (FT-IR, Nicolet 2005) and scanning electron microscopy (SEM, FEI Quanta 250). The samples were placed on a silicon wafer supported on copper stubs and coated with 10-nm thick gold dust prior to measurements. Concentrations of the rare earth ions were analyzed by Inductively Coupled Plasma Optical Emission Spectroscopy (ICP-OES, Optima 8000 DV, Perkin–Elmer, US).

2.3. Adsorption removal experiments

2.3.1. Effect of initial pH on the adsorption removal capacity of absorbents

0.1 g of absorbents were suspended in 50 mL light rare earth ions solutions (of Pr^{3+} and Nd^{3+}, respectively). The concentrations of Pr^{3+} and Nd^{3+} were 3.0 g/L. This selected concentration is attempted to simulate the high concentration of practical wastewater generated in rare earths mineral industry.

The pH of solutions was in the range of 2.0–6.0. The adsorption removal process was conducted at 40℃ with constant shaking for 1 h. Subsequently, the concentration of Pr^{3+} or Nd^{3+} in filtrate was analyzed by ICP-OES. The adsorption removal capacity was calculated from the concentrations of the two light rare earth ions before and after the adsorption.

2.3.2. Adsorption kinetics studies

The adsorption kinetics of the two light rare earth ions were conducted by suspending 0.1 g of absorbents in 50 mL of 3.0 g/L Pr^{3+} and Nd^{3+} solution, for which the pH was adjusted to 5.0. The adsorption process was conducted at 40℃ with constant shaking. The concentration of Pr^{3+} and Nd^{3+} were analyzed at regular intervals during the adsorption process.

2.3.3. Adsorption isotherm studies

Isotherm studies were carried out with initial concentrations of light rare earth ions ranging from 0.5 to 4.0 g/L. The pH of the solutions was adjusted to 5.0, which is the optimal pH. 0.1 g of absorbent was added into the solutions. The adsorption process was conducted with constant shaking at 40℃ for 1 h. Subsequently, the concentrations of Pr^{3+} and Nd^{3+} in the filtrate were analyzed.

3. Results and discussions

3.1. Preparation and characterization of absorbents

The preparation of SiO_2-BT, SiO_2-BWT and SiO_2-BT and BWT is illustrated in Fig. 1. Silica was usually used as support matrix due to its good chemical–physical properties [22]. Herein, we modified the silica with amino groups by the reverse micro-emulsion so that the plant polyphenols can further be chemically grafted onto silica.

There were large amount of adjacent phenolic hydroxyls on the B-rings of BT and BWT (Fig. 2), which exhibit specific affinity for many metal ions via forming five-member chelate ring [23]. Furthermore, the high nucleophilic reaction activity of C_6 in A-rings has endured BT and BWT the ability to form covalent bond with electrophilic chemicals, such as glutaraldehyde, which could react with amino groups on the surface of SiO_2 [24]. Thus, BT and BWT could be immobilized onto the aminated silica via Mannich reaction to prepare absorbents for the removal of rare earth ions [25].

3.2. Characterization of SiO_2-BT, SiO_2-BWT, and SiO_2-BT and BWT

FTIR spectra of the NH_2-SiO_2, SiO_2-BT, SiO_2-BWT, and SiO_2-BT and BWT are shown in Fig. 3. As shown in Fig. 3(a), the absorption band at 1,286.4 cm^{-1} is due to the stretching vibration of structural Si–O–Si of NH_2-SiO_2 and the band at 461.7 cm^{-1} is attributed to the Si–O–Si bending vibration [26,27]. The band at 3,425.4 cm^{-1} could be ascribed to the –OH bending vibration [28], which is located on the surface of silica. The absorption band at 786.6 cm^{-1} is assigned to the

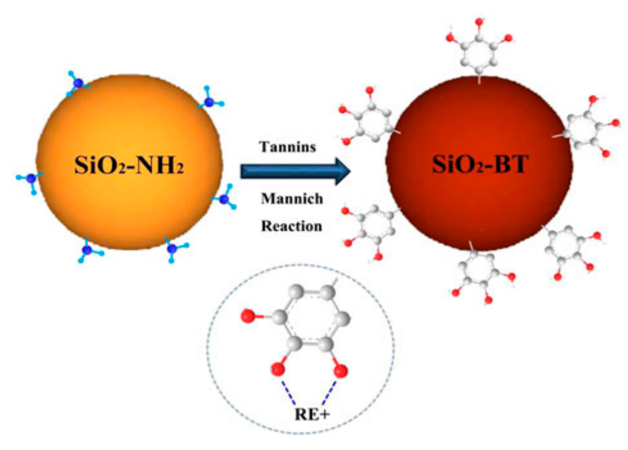

Fig. 1. Preparation of SiO_2-BT, SiO_2-BWT and SiO_2-BT and BWT.

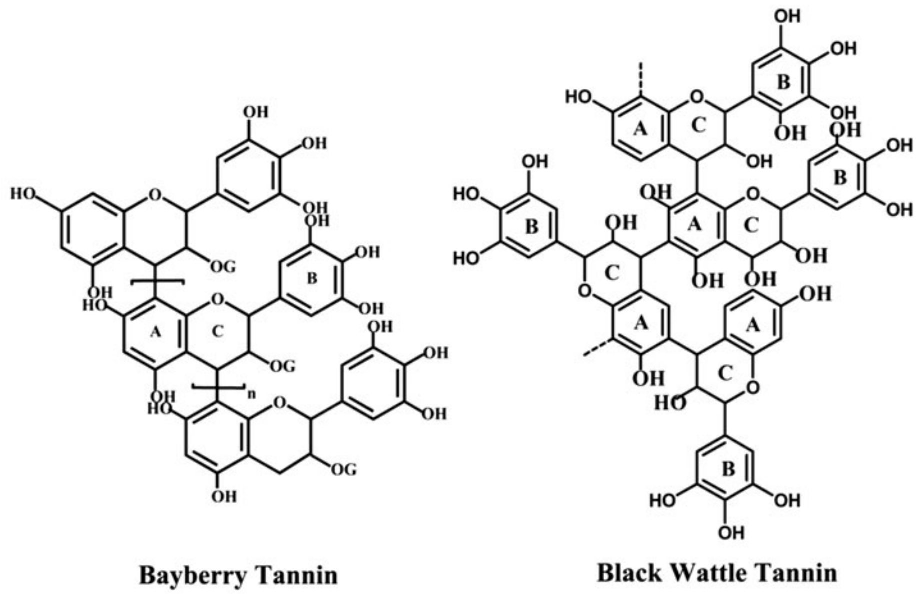

Fig. 2. Structures of bayberry tannin (BT) and black wattle tannin (BWT).

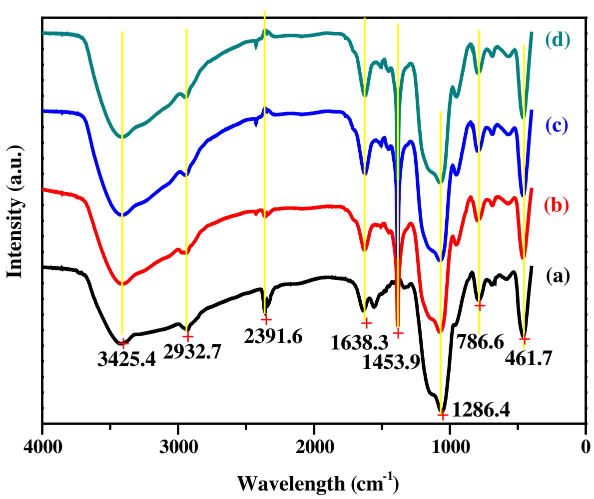

Fig. 3. FT-IR spectra of NH_2-SiO_2 (a), SiO_2-BT (b), SiO_2-BWT (c), and SiO_2-BT and BWT (d).

Si–OH stretching vibration. The band at 1,638.3 cm^{-1} is attributed to the HOH bending vibration [29], which results from H_2O in NH_2-SiO_2. In general, KH-550 in the sample was confirmed by the foregoing analysis. The results of elemental analysis show that the content of nitrogen in NH_2-SiO_2 is 5.767%, and the content of carbon is 16.005%, suggesting that the amino modification onto silica particles surface is achieved. The FTIR spectrum of SiO_2-BT is shown in Fig. 3(b). The absorption band at 1,286.4 cm^{-1} is assigned to asymmetric stretching vibration of structural Si–O–Si (in NH_2-SiO_2), and the band at 461.7 cm^{-1} is attributed to the Si–O–Si bending vibration [30]. The band at 3,425.3 cm^{-1} is due to the phenolic hydroxyl (in the molecule of BT) stretching vibration and the –OH (in NH_2-SiO_2) stretching vibration [31]. The absorption bands at 1,638.3 and 1,453.9 cm^{-1} are attributed to the benzene skeleton (in BT molecules) vibration. The adsorption band at 1,453.4 cm^{-1} is assigned to the phenolic hydroxyl in benzene ring, and the one at 2,932.7 cm^{-1} belongs to saturated C-H bond, indicating that the BT are grafted onto SiO_2. The absorption band of 3,425.4 cm^{-1} in Fig. 3(c) is due to the stretching vibration of hydroxyl in BWT molecule and SiO_2. The band at 2,932.6 cm^{-1} is attributed to saturated C–H bond stretching vibration [32]. The absorption bands at 1,628.3 and 1,453.5 cm^{-1} are attributed to the vibration of benzene rings in BWT molecules, suggesting that the BWT are grafted onto silica. The absorption bands in Fig. 3(d) confirm that the BT and BWT molecules are immobilized onto the SiO_2 matrix.

The SEM images of NH_2-SiO_2, SiO_2-BT, SiO_2-BWT and SiO_2-BT and BWT are shown in Fig. 4. It can be observed that the particle morphologies of SiO_2-BT, SiO_2-BWT, and SiO_2-BT and BWT have no significant changes compared with NH_2-SiO_2, which is formed from the aggregation of small particles of SiO_2-BT,

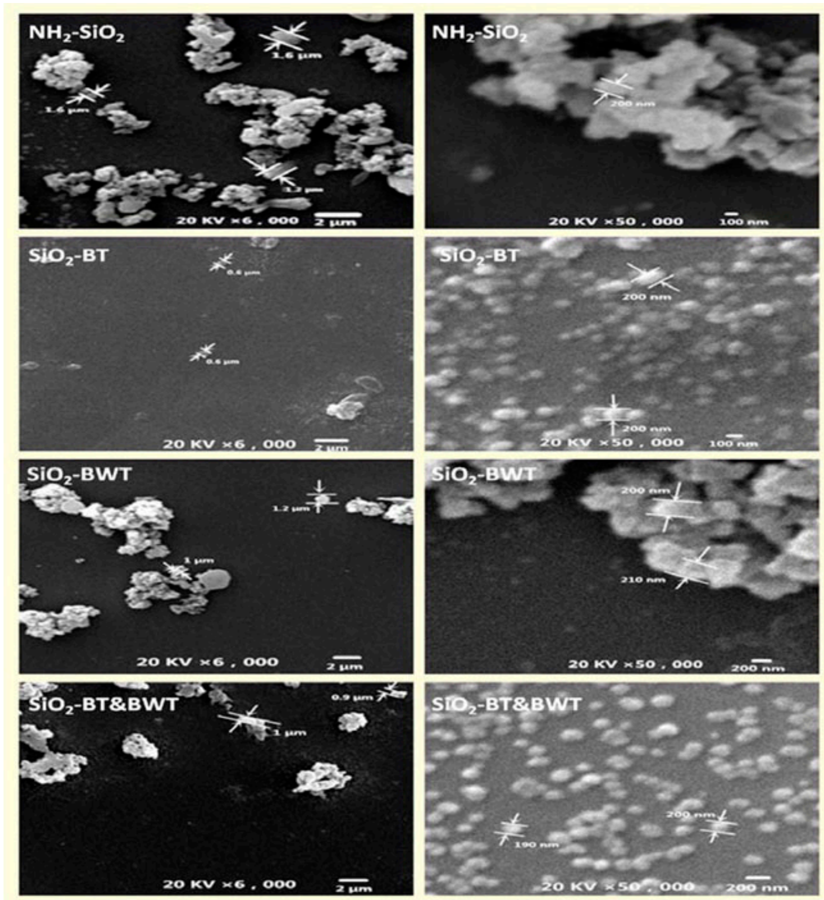

Fig. 4. SEM images of NH_2-SiO_2, SiO_2-BT, SiO_2-BWT, and SiO_2-BT and BWT.

SiO_2-BWT, SiO_2-BT and BWT. The most possible reason is that the hydrogen bonds could be formed between the hydroxyls of BT or BWT, which leads to the particle cluster observed by us [33].

3.3. Effect of pH

Fig. 5 shows the effect of initial pH on the adsorption capacity of adsorbents to the light rare earth ions. The optimal adsorption pH of SiO_2-BT to Pr^{3+} and Nd^{3+} are 4.0 and 5.0, respectively, while the optimal adsorption pH of SiO_2-BWT on Pr^{3+} and Nd^{3+} are 5.0 and 6.0, respectively. Both the optimal adsorption pH of SiO_2-BT and BWT to Pr^{3+} and Nd^{3+} are 5.0.

The dissociation degree of phenolic hydroxyls in BT and BWT should be influenced by the pH of solution [34]. When the pH of the solution is low, high concentrations of H^+ will restrain the dissociation of phenolic hydroxyls, resulting in a low adsorption capacity of Pr^{3+} and Nd^{3+}. In a solution with high pH, the dissociation of phenolic hydroxyls in BT and BWT will be promoted, thus showing high capacity of Pr^{3+} and Nd^{3+}.

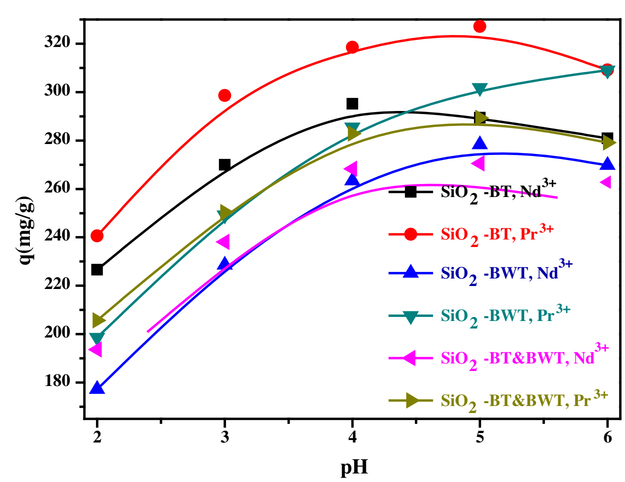

Fig. 5. Effect of initial pH on the adsorption capacity of light rare earth ions.

3.4. Adsorption kinetics

The effects of adsorption time on the adsorption capacity of Pr^{3+} and Nd^{3+} in a single system are shown in Fig. 6. The adsorption equilibrium of Pr^{3+} and Nd^{3+} on these adsorbents could be achieved around 60 min. At the beginning of the adsorption, the adsorption capacity is increased significantly. Subsequently, the adsorption capacity increases slowly in middle stage. Finally, it changes slightly and tends to reach the equilibrium with a platform. This fast adsorption kinetics could be attributed to the low mass transfer resistances, which has been greatly enhanced by the porous structures of the adsorbents (BT-SiO_2, SiO_2-BWT, SiO_2-BT and BWT). The porous structures provided both Pr^{3+} and Nd^{3+} easy access to the adsorption sites, resulting in high adsorption rate. The fast adsorption rate of Pr^{3+} and Nd^{3+} on these adsorbents (BT-SiO_2, SiO_2-BWT, SiO_2-BT and BWT) indicated that they could be suitable for the adsorptive recovery of Pr^{3+} and Nd^{3+} from large amount of solutions with appropriately diluted concentration.

The adsorption kinetics data were further fitted by the pseudo-second-order rate model, which was expressed in the following equation [35]:

$$t/q_t = (1/kq_e^2) + (1/q_e)t \quad (1)$$

where q_e and q_t are the adsorption capacity (mg/g) of Pr^{3+} and Nd^{3+} at equilibrium and at time t (min), respectively, and k (g/(mg min)) is the pseudo-second-order rate constant.

Good correlation coefficients ($R^2 > 0.99$) of these adsorption processes were obtained for the pseudo-second-order kinetics model.

3.5. Adsorption isotherms

Fig. 7 illustrates the experimental adsorption isotherms of these adsorbents (BT-SiO_2, SiO_2-BWT, SiO_2-BT and BWT) to Pr^{3+} and Nd^{3+}. When the concentrations of Pr^{3+} and Nd^{3+} are increased in the solutions, the adsorption capacities of these adsorbents are increased significantly at initial low concentration, and then, increased slowly thereafter.

Adsorption isotherms data were further fitted by Langmuir [36] and Freundlich [37] isothermal equations. The Langmuir (2) and Freundlich equations (3) are expressed as follows:

$$q_e = q_{max} bC_e/(1 + bC_e) \quad (2)$$

$$q_e = KC_e^{1/n} \quad (3)$$

where C_e is the equilibrium concentration (g/L), q_e is the equilibrium adsorption capacity (mg/g), q_{max} is the maximum adsorption capacity (mg/g), b and K are the Langmuir constant and the Freundlich constant, respectively.

It is shown in Fig. 7 that the Langmuir model provides a much better description to the isotherm data. The results fitted by Langmuir and Freundlich models are summarized in Table 1.

As shown in Table 1, the Langmuir equation gives satisfied fitting to the isotherm data with correlation constant (R^2) higher than 0.99. As for the gas–solid adsorption, the Langmuir isotherm model indicates a monolayer coverage of adsorbate over the homogeneous surface of adsorbent, and each molecule adsorbed on the surface has equal adsorption activa-

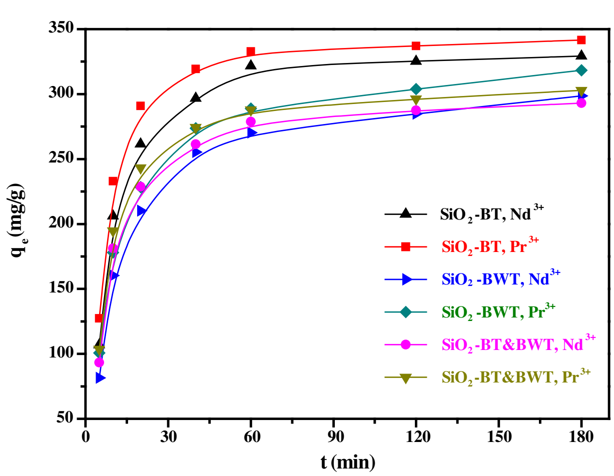

Fig. 6. Time effect on adsorption capacity of light rare earth ions.

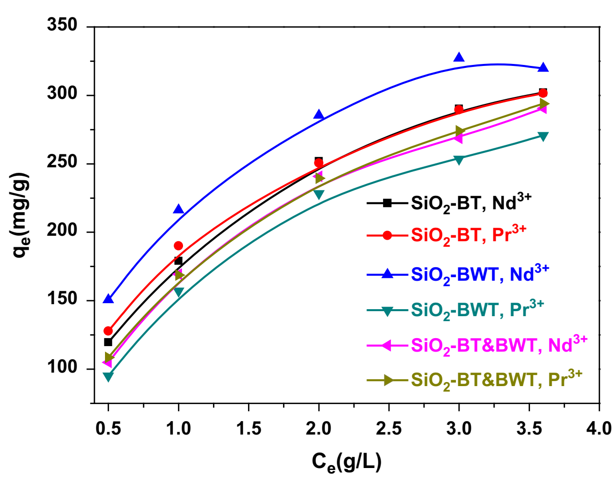

Fig. 7. The experimental adsorption isotherms of light rare earth ions.

Table 1
The Langmuir and Freundlich model parameters of the adsorption of light rare earth ions on these absorbents

		Langmuir				Freundlich		
Adsorbents	RE^{3+}	R^2	q_m	R_L	K_L	R^2	K_F	$1/n$
SiO_2-BT	Pr^{3+}	0.9965	344.83	0.118	0.0021	0.9880	20.086	0.3425
	Nd^{3+}	0.9958	357.14	0.082	0.0031	0.9783	33.784	0.2893
SiO_2-BWT	Pr^{3+}	0.9973	358.42	0.166	0.0014	0.9857	10.88	0.4155
	Nd^{3+}	0.9980	353.36	0.166	0.0014	0.9708	9.905	0.4265
SiO_2-BT and BWT	Pr^{3+}	0.9973	358.42	0.166	0.0014	0.9857	10.88	0.4155
	Nd^{3+}	0.9974	359.71	0.140	0.0017	0.9876	14.44	0.3852

tion energy, while the Freundlich isotherm model believes that the adsorption occurs on a heterogeneous surface of adsorbent. The above experimental results suggest that the phenolic hydroxyls grafted on the surface of SiO_2 should have even distribution and play equal role as active adsorptive sites regardless of their locations. Therefore, Pr^{3+} and Nd^{3+} may be adsorbed in the form of monolayer on the surfaces of SiO_2-BT, SiO_2-BWT, and SiO_2-BT and BWT, respectively.

4. Conclusion

In the present investigation, bayberry tannin-immobilized aminated silica (SiO_2-BT), black wattle tannin-immobilized aminated silica (SiO_2-BWT) and bayberry tannin and black wattle tannin-immobilized aminated silica (SiO_2-BT and BWT) have been successfully synthesized and applied for the removal of Pr^{3+} and Nd^{3+} from aqueous solutions. It was found that SiO_2-BT showed the best adsorption performances for the removal of both Pr^{3+} and Nd^{3+} in aqueous solutions among these absorbents. Under optimum conditions, the adsorption equilibrium was achieved within 60 min, showing extremely fast adsorption kinetics. The adsorption capacity of SiO_2-BT to Pr^{3+} and Nd^{3+} was 329.2 and 341.5 mg/g, respectively. The adsorption kinetics was adequately described by the pseudo-second-order kinetic equations, while the adsorption isotherms followed the Langmuir equations. In conclusion, SiO_2-BT is suitable for the effective removal of Pr^{3+} and Nd^{3+} from aqueous solutions.

Acknowledgments

This project were supported by the National Natural Science Foundation of China (511713122; 21406147; 51079166) and Science and Technology Project of Chengdu (2014-HM01-00204-SF; 2014-HM01-00205-SF).

References

[1] A. Saguchi, T. Uesugi, Y. Takigawa, K. Higashi, Development of highly efficient saving processes of rare earth in R-T-B permanent magnet, Phys. Proc. 54 (2014) 168–173.
[2] L. Lekha, K.K. Raja, G. Rajagopal, D. Easwaramoorthy, Schiff base complexes of rare earth metal ions: Synthesis, characterization and catalytic activity for the oxidation of aniline and substituted anilines, J. Organomet. Chem. 753 (2014) 72–80.
[3] D. Yadav, R. Kripal, P. Gnutek, C. Rudowicz, Systematization of crystal field parameters for trivalent rare-earth (RE^{3+}) ions at orthorhombic sites in selected laser materials—Standardization approach, J. Phys. Chem. Solids 74 (2013) 751–758.
[4] M. Amsif, D. Marrero-Lopez, J.C. Ruiz-Morales, S.N. Savvin, M. Gabás, P. Nunez, Influence of rare-earth doping on the microstructure and conductivity of $BaCe_{0.9}Ln_{0.1}O_{3-\delta}$ proton conductors, J. Power Sources 196 (2011) 3461–3469.
[5] D. Das, C. Jaya Sre Varshini, N. Das, Recovery of lanthanum(III) from aqueous solution using biosorbents of plant and animal origin: Batch and column studies, Miner. Eng. 69 (2014) 40–56.
[6] C.H. Xiong, X.Y. Chen, C.P. Yao, Enhanced adsorption behavior of Nd(III) onto D113-III resin from aqueous solution, J. Rare Earths 29 (2011) 979–985.
[7] K. Vijayaraghavan, M. Sathishkumar, R. Balasubramanian, Interaction of rare earth elements with a brown marine alga in multi-component solutions, Desalination 265 (2011) 54–59.
[8] M. Husain, S.A. Ansari, P.K. Mohapatra, R.K. Gupta, V.S. Parmar, V.K. Manchanda, Extraction chromatography of lanthanides using N,N,N´,N´-tetraoctyl diglycolamide (TODGA) as the stationary phase, Desalination 229 (2008) 294–301.
[9] G.S. Lee, M. Uchikoshi, K. Mimura, M. Isshiki, Distribution coefficients of La, Ce, Pr, Nd, and Sm on Cyanex 923-, D2EHPA-, and PC88A-impregnated resins, Sep. Purif. Technol. 67 (2009) 79–85.
[10] C.H. Xiong, C.P. Yao, Preparation and application of acrylic acid grafted polytetrafluoroethylene fiber as a weak acid cation exchanger for adsorption of Er(III), J. Hazard. Mater. 170 (2009) 1125–1132.
[11] G.A. Moldoveanu, V.G. Papangelakis, Recovery of rare earth elements adsorbed on clay minerals: I.

Desorption mechanism, Hydrometallurgy 117–118 (2012) 71–78.
[12] J. Beltrán-Heredia, J. Sánchez-Martín, G. Frutos-Blanco, *Schinopsis balansae* tannin-based flocculant in removing sodium dodecyl benzene sulfonate, Sep. Purif. Technol. 67 (2009) 295–303.
[13] M. Gurung, B.B. Adhikari, S. Morisada, H. Kawakita, K. Ohto, K. Inoue, S. Alam, N-aminoguanidine modified persimmon tannin: A new sustainable material for selective adsorption, preconcentration and recovery of precious metals from acidic chloride solution, Bioresour. Technol. 129 (2013) 108–117.
[14] M. Gurung, B.B. Adhikari, H. Kawakita, K. Ohto, K. Inoue, S. Alam, Recovery of gold and silver from spent mobile phones by means of acidothiourea leaching followed by adsorption using biosorbent prepared from persimmon tannin, Hydrometallurgy 133 (2013) 84–93.
[15] K. Banu, T. Shimura, S. Sadeghi, Selective detection and recovery of gold at tannin-immobilized non-conducting electrode, Anal. Chim. Acta 853 (2015) 207–213.
[16] A. Nakajima, T. Sakaguchi, Recovery of uranium by tannins immobilized on agarose, J. Chem. Technol. Biotechnol. 40 (1987) 223–232.
[17] L. Lima, S. Olivares, F. Martínez, J. Torres, D. de la Rosa, C. Sepúlveda, Use of immobilized tannin adsorbent for removal of Cr(VI) from water, J. Radioanal. Nucl. Chem. 231 (1998) 35–40.
[18] A. Kazemi, M.A. Faghihi-Sani, M.J. Nayyeri, M. Mohammadi, M. Hajfathalian, Effect of zircon content on chemical and mechanical behavior of silica-based ceramic cores, Ceram. Int. 40 (2014) 1093–1098.
[19] M.R. Mahmoud, G.E. Sharaf El-deen, M.A. Soliman, Surfactant-impregnated activated carbon for enhanced adsorptive removal of Ce(IV) radionuclides from aqueous solutions, Ann. Nucl. Energy 72 (2014) 134–144.
[20] L.L. Zhu, J. Chen, Adsorption of Ce(IV) in nitric acid medium by imidazolium anion exchange resin, J. Rare Earths 29 (2011) 969–973.
[21] X. Huang, Y.P. Wang, X.P. Liao, B. Shi, Adsorptive recovery of Au^{3+} from aqueous solutions using bayberry tannin-immobilized mesoporous silica, J. Hazard. Mater. 183 (2010) 793–798.
[22] T. Takei, T. Konishi, M. Fuji, T. Watanabe, M. Chikazawa, Phase transition of capillary condensed liquids in porous silica: effect of surface hydroxyl groups, Thermochim. Acta 267 (1995) 159–167.
[23] C.W. Oo, M.J. Kassim, A. Pizzi, Characterization and performance of *Rhizophora apiculata* mangrove polyflavonoid tannins in the adsorption of copper(II) and lead(II), Ind. Crop. Prod. 30 (2009) 152–161.
[24] X.Y. Guo, H.Q. Shao, W.L. Hu, W. Gao, X. Chen, Tannin and polyacrylic acid polarity and structure influence on the performance of polyvinylchloride ultrafiltration membrane, Desalination 250 (2010) 740–744.
[25] B. Lal, V.G. Gund, N.B. Bhise, A.K. Gangopadhyay, Mannich reaction: An approach for the synthesis of water soluble mulundocandin analogues, Bioorg. Med. Chem. 12 (2004) 1751–1768.
[26] J.B. Kim, I. Sohn, Influence of TiO_2/SiO_2 and MnO on the viscosity and structure in the TiO_2–MnO–SiO_2 welding flux system, J. Non-Cryst. Solids 379 (2013) 235–243.
[27] Z. Li, B. Hou, Y. Xu, D. Wu, Y. Sun, Hydrothermal synthesis, characterization, and photocatalytic performance of silica-modified titanium dioxide nanoparticles, J. Colloid Interface Sci. 288 (2005) 149–154.
[28] S. Jothivel, R. Velmurugan, K. Selvam, B. Krishnakumar, M. Swaminathan, Preparation, characterization and photocatalytic activity of acidic sulfated nano titania for the degradation of Reactive Orange 4 under UV light, Sep. Purif. Technol. 77 (2011) 245–250.
[29] E. Horváth, J. Kristóf, H. Nasser, R.L. Frost, A. De Battisti, Á. Rédey, Investigation of SnO_2 thin film evolution by thermoanalytical and spectroscopic methods, Appl. Surf. Sci. 242 (2005) 13–20.
[30] F. Prinetto, G. Ghiotti, M. Occhiuzzi, V. Indovina, Characterization of oxidized surface phases on VO_x/ZrO_2 catalysts, J. Phys. Chem. B 102 (1998) 10316–10325.
[31] M. Guidotti, N. Ravasio, R. Psaro, G. Ferraris, G. Moretti, Epoxidation on titanium-containing silicates: Do structural features really affect the catalytic performance? J. Catal. 214 (2003) 242–250.
[32] G.A. Pitsevich, A.E. Malevich, E.N. Kozlovskaya, I.Yu. Doroshenko, V.E. Pogorelov, V. Sablinskas, V. Balevicius, Theoretical study of the C–H/O–H stretching vibrations in malonaldehyde, Spectrochim. Acta, Part A 145 (2015) 384–393.
[33] S.R. Kirk, D. Yin, M. Persson, J. Carlen, S. Jenkins, Molecular dynamics simulations of the aggregation of nanocolloidal amorphous silica monomers and dimers, Proc. Eng. 18 (2011) 188–193.
[34] J. Sánchez-Martín, M. González-Velasco, J. Beltrán-Heredia, J. Gragera-Carvajal, J. Salguero-Fernández, Novel tannin-based adsorbent in removing cationic dye (Methylene Blue) from aqueous solution. Kinetics and equilibrium studies, J. Hazard. Mater. 174 (2010) 9–16.
[35] Y.S. Ho, G. McKay, Pseudo-second order model for sorption processes, Process Biochem. 34 (1999) 451–465.
[36] I. Langmuir, The constitution and fundamental properties of solids and liquids. Part I. Solids, J. Am. Chem. Soc. 38 (1916) 2221–2295.
[37] G. Gamez, J.L. Gardea-Torresdey, K.J. Tiemann, J. Parsons, K. Dokken, M.J. Jose Yacaman, Recovery of gold(III) from multi-elemental solutions by alfalfa biomass, Adv. Environ. Res. 7 (2003) 563–571.